OncoTargets and Therapy

Dovepress
open access to scientific and medical research

Open Access Full Text Article

ORIGINAL RESEARCH

Integrated Analysis To Identify Molecular Biomarkers Of High-Grade Serous Ovarian Cancer

This article was published in the following Dove Press journal:
OncoTargets and Therapy

Manfei Si[1]
Junji Zhang[1]
Jianzhong Cao[2]
Zhibo Xie[3]
Shan Shu[1]
Yapei Zhu[1]
Jinghe Lang[1]

[1]Department of Obstetrics and Gynecology, Peking Union Medical College Hospital, Peking Union Medical College, Chinese Academy of Medical Sciences, Beijing, People's Republic of China; [2]Department of General Surgery, Peking Union Medical College Hospital, Peking Union Medical College, Chinese Academy of Medical Sciences, Beijing, People's Republic of China; [3]Department of Vascular Surgery, Peking Union Medical College Hospital, Peking Union Medical College, Chinese Academy of Medical Sciences, Beijing, People's Republic of China

Purpose: Ovarian cancer is the leading cause of gynecologic cancer-related death worldwide. Early diagnosis of ovarian cancer can significantly improve patient prognosis. Hence, there is an urgent need to identify key diagnostic and prognostic biomarkers specific for ovarian cancer. Because high-grade serous ovarian cancer (HGSOC) is the most common type of ovarian cancer and accounts for the majority of deaths, we identified potential biomarkers for the early diagnosis and prognosis of HGSOC.

Methods: Six datasets (GSE14001, GSE18520, GSE26712, GSE27651, GSE40595, and GSE54388) were downloaded from the Gene Expression Omnibus database for analysis. Differentially expressed genes (DEGs) between HGSOC and normal ovarian surface epithelium samples were screened via integrated analysis. Hub genes were identified by analyzing protein–protein interaction (PPI) network data. The online Kaplan-Meier plotter was utilized to evaluate the prognostic roles of these hub genes. The expression of these hub genes was confirmed with Oncomine datasets and validated by quantitative real-time PCR and Western blotting.

Results: A total of 103 DEGs in patients with HGSOC—28 upregulated genes and 75 downregulated genes—were successfully screened. Enrichment analyses revealed that the upregulated genes were enriched in cell division and cell proliferation and that the downregulated genes mainly participated in the Wnt signaling pathway and various metabolic processes. Ten hub genes were associated with HGSOC pathogenesis. Seven overexpressed hub genes were partitioned into module 1 of the PPI network, which was enriched in the cell cycle and DNA replication pathways. Survival analysis revealed that *MELK, CEP55* and *KDR* expression levels were significantly correlated with the overall survival of HGSOC patients ($P < 0.05$). The RNA and protein expression levels of these hub genes were validated experimentally.

Conclusion: Based on an integrated analysis, we propose the further investigation of *MELK, CEP55* and *KDR* as promising diagnostic and prognostic biomarkers of HGSOC.

Keywords: high-grade serous ovarian cancer, integrated analysis, bioinformatic analysis, differentially expressed genes, survival, biomarker

Introduction

Ovarian cancer is the leading cause of gynecologic cancer-related death and the fifth most common cause of cancer death in the United States. In 2018, approximately 22,240 new ovarian carcinoma cases and 14,070 associated deaths were expected in the United States, corresponding to almost 39 deaths per day.[1] Because of the location of the ovaries and the lack of symptoms of early-stage disease, approximately 70% of ovarian cancer patients present with advanced disease (FIGO stage III/IV) and have a poor prognosis.[1–4] In contrast, if ovarian cancer could be

Correspondence: Jinghe Lang
Department of Obstetrics and Gynecology, Peking Union Medical College Hospital, Peking Union Medical College, Chinese Academy of Medical Sciences, No. 1 Shuaifuyuan, Dongcheng District, Beijing 100730, People's Republic of China
Tel +86 10 6915 6204
Email langjh@hotmail.com

diagnosed at a local stage, the 5-year relative survival rate would exceed 90%.[1,2] Hence, there is an urgent need to identify key early diagnostic and prognostic biomarkers specific for ovarian cancer that could significantly impact patient survival.

Approximately ninety percent of ovarian cancers are epithelial ovarian cancers (EOCs), which are divided into four main histologic subtypes—serous, mucinous, endometrioid, and clear cell.[3,5–7] The vast majority (70%) of EOCs are serous.[8] Serous ovarian cancer can be categorized as high-grade serous ovarian cancer (HGSOC, grade 2 or 3) or low-grade serous ovarian cancer (LGSOC, grade 1), which have different pathogeneses and clinicopathologic features.[9–13] HGSOC is the most common type of EOC and has aggressive behavior, thereby accounting for the majority of deaths. Thus, we focused on HGSOC in this study.

Recent advances in microarray-based profiling and high-throughput biological sequencing technologies have yielded considerable abilities to identify differentially expressed genes (DEGs) and discover potential biological mechanisms, thus allowing the identification of promising biomarkers for cancer diagnosis, treatment and prognosis. In this study, gene expression profiling data for human HGSOC and normal ovarian surface epithelium (OSE) samples were used to identify DEGs and analyzed their underlying biological functions by functional and pathway enrichment analyses. Then, protein-protein interaction (PPI) networks and Cytoscape were utilized to identify the hub genes, which were found to be closely related to the pathogenesis and progression of HGSOC; thus, these genes may play a vital role in the early diagnosis of HGSOC. Finally, the prognostic value of the hub genes in HGSOC was further confirmed by survival analysis, which can be used to identify predictors of poor clinical outcomes for patients with HGSOC. A flowchart of the analysis process is shown in Figure 1.

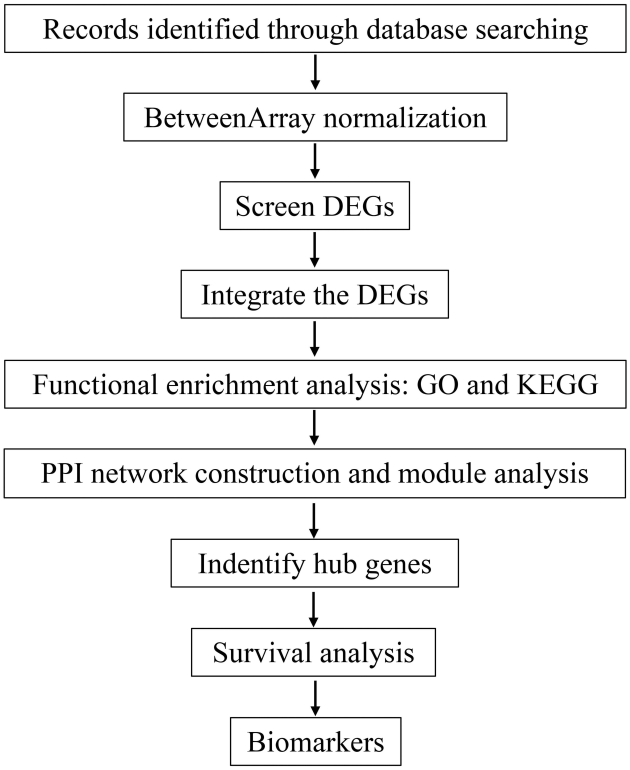

Figure 1 Flowchart of the analysis process.
Abbreviations: DEGs, differentially expressed genes; GO, Gene Ontology; KEGG, Kyoto Encyclopedia of Genes and Genomes; PPI, protein-protein interaction.

Materials And Methods

Gene Expression Profiling Data

Gene expression microarray data (GSE14001, GSE18520, GSE26712, GSE27651, GSE40595, and GSE54388) were downloaded from the National Center for Biotechnology Information Gene Expression Omnibus (GEO) database (http://www.ncbi.nlm.nih.gov/geo/). All included datasets met the following criteria: (1) they contained human HGSOC and normal OSE tissue samples; (2) the data were subjected to expression profiling by array analysis; and (3) they contained at least ten samples. These profile datasets were based on the Affymetrix GPL570 platform (Affymetrix Human Genome U133 Plus 2.0 Array), except for GSE26712, which was based on the Affymetrix GPL96 platform (Affymetrix Human Genome U133A Array). Six datasets including a total of 359 tissue samples (318 HGSOC samples and 41 normal OSE samples) were chosen for analysis.

Integrated Analysis Of Microarray Datasets

Raw data from GSE14001, GSE18520 and GSE27651 were first subjected to base 2 logarithmic conversion for further analysis in R software. The BetweenArray normalization function in the limma package of R was applied to normalize the matrix data from each GEO dataset.[14] After normalization, DEGs between HGSOC and OSE were screened by using empirical Bayes methods within the limma package.[15] Based on the robust rank aggregation (RRA) method,[16] the RobustRankAggreg package in R was utilized to integrate the DEGs identified in the six

datasets. The following threshold values were established for screening DEGs: $|\log_2 FC| \geq 2$, where FC is the fold change; adjusted $P < 0.05$; and $P < 0.05$.

Functional Enrichment Analysis Of DEGs

We performed Gene Ontology (GO) enrichment analysis of the DEGs using the Database for Annotation, Visualization and Integrated Discovery (DAVID, version 6.8) (http://string-db.org/).[17] GO analysis annotates genes with respect to three independent ontologies—biological process (BP), cellular component (CC), and molecular function (MF).[18] To elucidate potential pathways associated with the DEGs, Kyoto Encyclopedia of Genes and Genomes (KEGG) pathway enrichment analysis was conducted in the clusterProfiler package[19] to annotate genes with pathways.[20] The false discovery rate (FDR) was obtained by adjusting the P value according to the Benjamini-Hochberg method.[21] Genes with $P < 0.05$ and adjusted $P < 0.05$ or FDR < 0.05 were considered statistically significant.

PPI Network Construction And Module Analysis

The STRING online database (version 11.0) (http://string-db.org/) was used to assess potential interactions among the DEGs.[22] PPIs with an interaction score ≥ 0.4 (medium confidence) were utilized to construct the PPI network. Cytoscape software (version 3.7.0) was used to visualize and analyze the degree of connectivity to identify hub genes in the PPI networks.[23] According to the degree of connectivity,[24] we screened the top 10 hub genes. To detect the densely connected protein complexes in the PPI network, the Molecular Complex Detection (MCODE) app from Cytoscape was utilized with the default parameters to identify modules.[25] Then, for significant module 1, we performed further GO and KEGG pathway enrichment analyses as previously described.

Survival Analysis

The Kaplan-Meier Plotter website (www.kmplot.com/ovar) was utilized to validate the prognostic role of the ten hub genes in ovarian cancer patients. This website includes data for 2190 ovarian cancer samples on Affymetrix microarrays.[26] We selected survival information for patients with HGSOC (grades 2 and 3) from multiple datasets (all available on the website) for the analysis.[27] The patients were divided into two groups based on the best cutoff for gene expression (high vs low). The overall survival (OS) rates of the two groups were analyzed and Kaplan-Meier survival plots were then generated. Then, we performed a subgroup analysis considering stage, grade, TP53 mutation and treatment to understand how the expression of the identified hub genes impacts OS. Hazard ratios (HRs) with 95% confidence intervals (CIs) were calculated to identify protective (HR < 1) or risk genes (HR > 1), and the survival curves were plotted to visualize the relationships. A log rank $P < 0.05$ was set as the cutoff criterion.

Validation Of Key Genes

Hub genes were identified as the top 10 nodes in the PPI network. To confirm the reliability of these detected genes, we evaluated their expression in ovarian serous adenocarcinoma and normal ovarian tissues using datasets from Oncomine (www.oncomine.org). In addition, the expression of the ten hub genes was experimentally validated by quantitative real-time PCR (qRT-PCR). Among the hub genes, EPCAM (epithelial cell adhesion molecule), ZWINT (ZW10-interacting kinetochore protein), DLGAP5 (DLG-associated protein 5) and KDR (kinase insert domain receptor) protein expression levels were confirmed by Western blotting.

Clinical Samples

With the approval of the Ethics Review Committee of Peking Union Medical College Hospital, Chinese Academy of Medical Sciences (ZS-1771), twenty-two HGSOC and twenty-two normal ovarian tissue samples were collected during initial operations between 2017 and 2018. All subjects gave written informed consent in accordance with the Declaration of Helsinki. HGSOC samples were obtained from primary ovarian cancer patients who had not previously received chemotherapy. Normal ovarian tissues were obtained from patients who underwent a total hysterectomy and bilateral salpingo-oophorectomy for benign uterine diseases (uterine prolapse or uterine leiomyoma) or precancerous lesions of the uterine cervix. Table 1 summarizes the clinicopathological characteristics of the patients with HGSOC included in the study. All tissue specimens were pathologically confirmed before inclusion. All the fresh samples were frozen in liquid nitrogen and stored at −80°C.

RNA Isolation And qRT-PCR

Total RNA was extracted using TRIzol Reagent (Invitrogen) according to the manufacturer's protocol. After the RNA concentration was measured with the Genova Nano

Table 1 Clinicopathological Characteristics Of The Patients With HGSOC Included In The Study

Patient	Age, y	Histology Type	Grade	FIGO Stage	Residual	Lymphectomy	Lymph Nodes Metastasis
1	41	Serous	High	IIIC	Yes	No	NA
2	53	Serous	High	IIIC	Yes	No	NA
3	55	Serous	High	IV	Yes	Yes	+
4	51	Serous	High	III	No	Yes	–
5	38	Serous	High	IA	NA	Yes	–
6	55	Serous	High	IC	No	Yes	–
7	63	Serous	High	IIIC	Yes	No	NA
8	53	Serous	High	II	Yes	No	NA
9	50	Serous	High	IV	No	Yes	+
10	80	Serous	High	IIIC	Yes	No	NA
11	40	Serous	High	III	Yes	Yes	+
12	51	Serous	High	IIIC	Yes	Yes	+
13	63	Serous	High	III	Yes	No	NA
14	50	Serous	High	IIB	No	Yes	–
15	49	Serous	High	IIIC	Yes	Yes	+
16	48	Serous	High	IIIB	Yes	Yes	–
17	63	Serous	High	III	Yes	No	NA
18	59	Serous	High	IIIB	Yes	Yes	–
19	65	Serous	High	IV	No	Yes	–
20	52	Serous	High	III	No	Yes	+
21	62	Serous	High	IV	Yes	No	NA
22	56	Serous	High	III	NA	Yes	+

Micro-volume Spectrophotometer (Jenway), cDNA was synthesized using GoScript™ Reverse Transcriptase (Promega). qRT-PCR was performed using GoTaq® qPCR (Promega) with the LightCycler® 480 System (Roche) in accordance with the manufacturer's instructions. The qRT-PCR primers are shown in Supplementary Table 1. The conditions for all qRT-PCRs were as follows: Hot Start Taq activation for 1 min at 95°C, followed by 45 cycles of 95°C for 10 seconds, 58°C for 15 seconds and 72°C for 15 seconds, with a final step at 55°C for 1 min. The relative expression of target genes was calculated by the $2^{-\triangle\triangle Ct}$ method using GAPDH as the internal control.

Western Blot Analysis

Tissues were lysed in RIPA buffer with Halt™ Protease and Phosphatase Inhibitor Cocktail (Thermo Scientific). Protein concentration was determined by the Bradford method using the Enhanced BCA Protein Assay Kit (Beyotime). Equal amounts of protein from each sample were separated in NuPAGE™ 4–12% Bis-Tris Protein Gels (Invitrogen) and transferred to PVDF membranes (0.2 μm pore size) using iBlot® 2 Transfer Stacks (Invitrogen). After being blocked with 5% nonfat milk in TBS with 0.1% Tween 20 for 1 hr at room temperature, the membranes were incubated overnight at 4°C with primary antibodies against the following proteins: EPCAM (1:1000; Cell Signaling #2929), ZWINT (1:2000; Abcam #71982), DLGAP5 (hepatoma upregulated protein, HURP; 1:2000, Abcam #70744), KDR (VEGFR2, 1:1000; Cell Signaling #2479) and β-actin (1:2000; ZSGB-BIO #TA-09). The membranes were subsequently incubated with a horseradish peroxidase (HRP)-conjugated secondary antibody at room temperature for 1 hr. Then, immunoreactive bands were detected with Immobilon Western Chemiluminescent HRP substrate (Millipore).

Statistical Analysis

GraphPad Prism 6.0 software was used to analyze the experimental data. The results are shown as the mean ± SEM. The statistical significance of differences between two groups was evaluated using Student's *t*-test (two-tailed). $P < 0.05$ was considered to indicate statistical significance.

Results

Identification Of DEGs

Information on the six GEO datasets included in the current study is provided in Table 2.[28–34] The six datasets included a total of 318 HGSOC samples and 41 normal OSE

Table 2 Information On The Six GEO Datasets Included In The Current Study

Dataset	Reference	Platform		Number Of Samples (HGSOC/OSE)
GSE14001	Tung et al[28]	GPL570	[HG-U133_Plus_2] Affymetrix Human Genome U133 Plus 2.0 Array	13 (10/3)
GSE18520	Mok et al[29]	GPL570	[HG-U133_Plus_2] Affymetrix Human Genome U133 Plus 2.0 Array	63 (53/10)
GSE26712	Bonome et al[30] Vathipadiekal et al[31]	GPL96	[HG-U133A] Affymetrix Human Genome U133A Array	195 (185/10)
GSE27651	King et al[32]	GPL570	[HG-U133_Plus_2] Affymetrix Human Genome U133 Plus 2.0 Array	28 (22/6)
GSE40595	Yeung et al[33]	GPL570	[HG-U133_Plus_2] Affymetrix Human Genome U133 Plus 2.0 Array	38 (32/6)
GSE54388	Yeung et al[34]	GPL570	[HG-U133_Plus_2] Affymetrix Human Genome U133 Plus 2.0 Array	22 (16/6)

Abbreviations: HGSOC, high-grade serous ovarian cancer; OSE, ovarian surface epithelium.

samples. Supplementary Table 2 presents detailed information on the samples in each included dataset. The data from each GEO dataset were normalized, and the results are presented in Supplementary Figure 1. Using $|\log_2 FC| \geq 2$, adjusted $P < 0.05$ and $P < 0.05$ as cutoff criteria, we successfully screened a total of 103 DEGs via integrated analysis of the six GEO datasets (Supplementary Table 3). Of the 103 DEGs, 28 were significantly upregulated and 75 were downregulated in HGSOC tissues compared to normal OSE tissues. The DEGs obtained from each GEO dataset are shown in Figure 2. Figure 3 presents the 103 DEGs identified by integrated analysis of the six GEO datasets

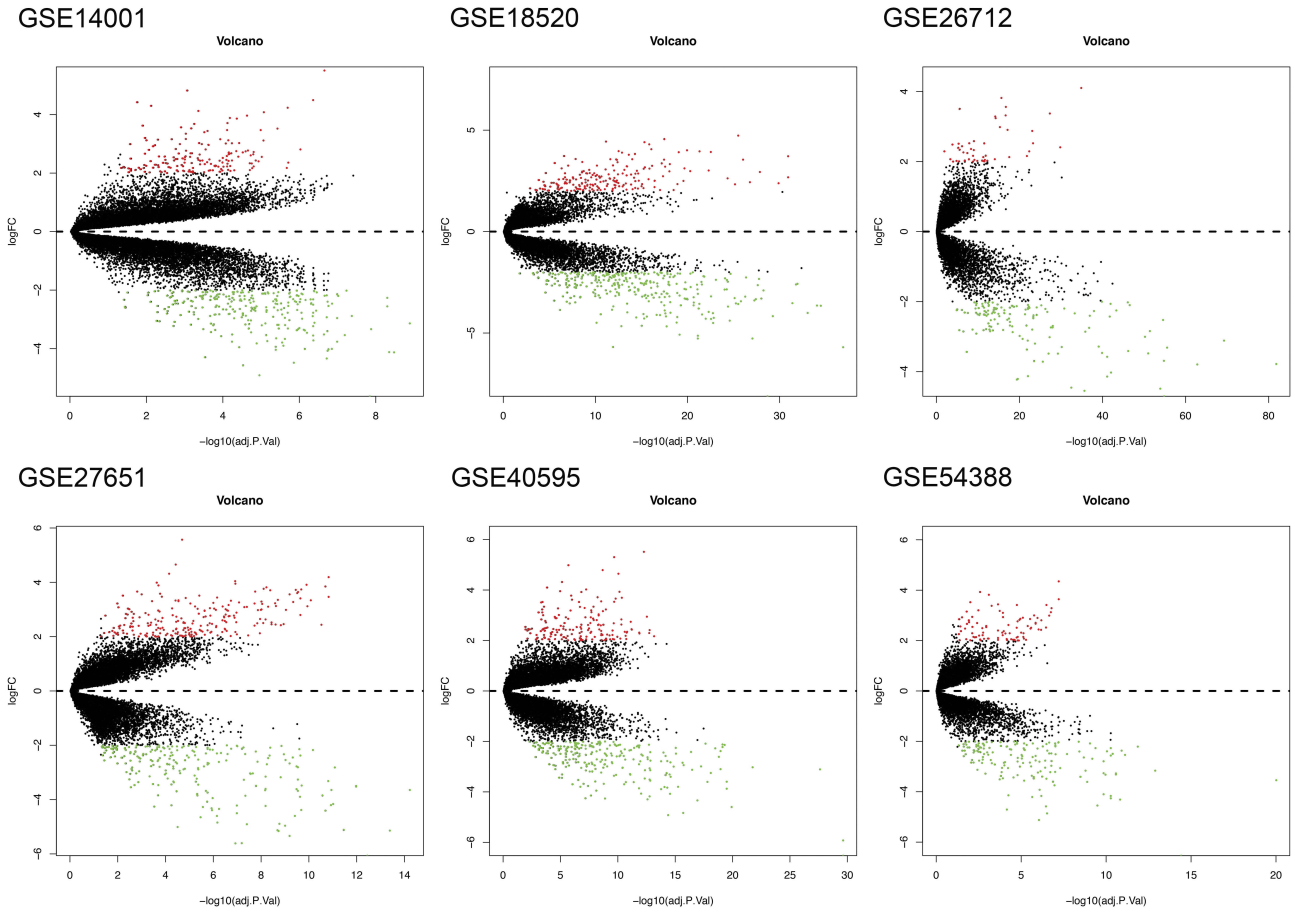

Figure 2 DEGs obtained from each GEO dataset (GSE14001, GSE18520, GSE26712, GSE27651, GSE40595, and GSE54388). The red points represent upregulated genes screened with $|\log_2 FC| \geq 2$ and adjusted $P < 0.05$. The green points represent downregulated genes screened with $|\log_2 FC| \geq 2$ and adjusted $P < 0.05$. The black points represent genes with no significant difference in expression.
Abbreviations: DEGs, differentially expressed genes; GEO, Gene Expression Omnibus; FC, fold change.

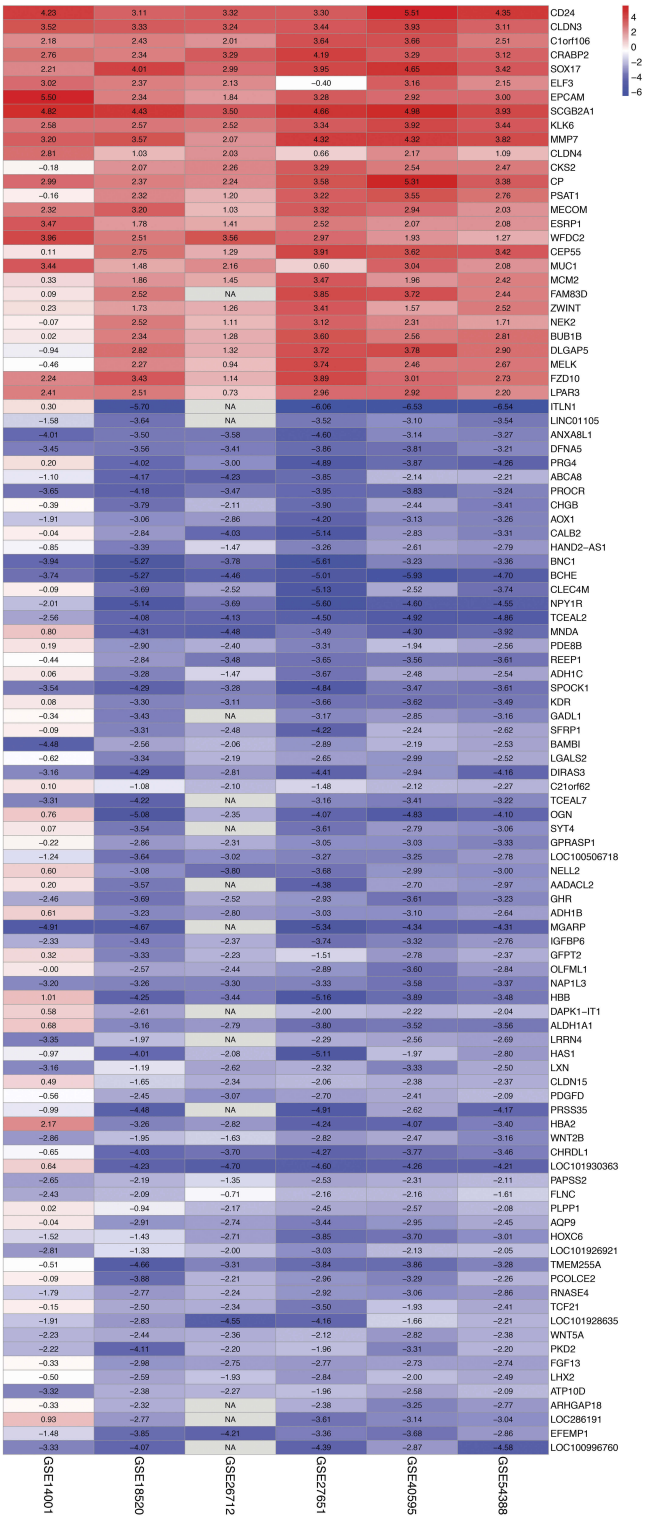

Figure 3 Heat map of the 103 DEGs identified in the integrated microarray analysis. Each column represents one dataset, and each row represents one gene. The number in each rectangle is the log_2FC value. The color gradient from blue to red represents the progression from down- to upregulation.
Abbreviations: DEGs, differentially expressed genes; FC, fold change.

based on the RRA method. Supplementary Figure 2 shows the heat map of these 103 integrated DEGs in HGSOC and normal OSE tissues acquired from the GEO datasets. Supplementary Table 4 shows the detailed expression data for each included sample.

Functional Enrichment Analysis Of The DEGs

GO enrichment analysis for the three GO categories (BP, CC and MF) was performed in DAVID. As shown in Figure 4A, a total of nine GO terms with $P < 0.05$ and FDR < 0.05 were enriched (Supplementary Table 5). The 28 upregulated genes were significantly enriched in multiple BPs related to cell division and cell proliferation. The 75 downregulated genes were closely correlated with the ethanol oxidation term in the BP category; the extracellular region, proteinaceous extracellular matrix and extracellular exosome terms in the CC category; and the frizzled binding term in the MF category. Subsequently, we conducted KEGG pathway analysis the integrated 103 DEGs with the clusterProfiler package to explore potential enriched pathways. The downregulated genes mainly participated in the Wnt signaling pathway and diverse metabolism-associated signaling pathways, such as retinol metabolism, tyrosine metabolism, and drug metabolism/cytochrome P450 (Figure 4B and Supplementary Table 6). However, significantly enriched KEGG pathways were not identified for the upregulated genes.

PPI Network Construction And Module Analysis

The STRING website was used to filter a total of 99 DEGs (28 upregulated and 71 downregulated) with a combined interaction score of > 0.4 and construct the PPI network, which comprised 65 nodes and 226 interactions (Figure 5A and Supplementary Table 7). The NetworkAnalyzer app in Cytoscape was used to calculate the node degrees to identify hub genes.[23] After analyzing the data from STRING using the NetworkAnalyzer app, we screened the top 10 hub nodes according to node degree.[24] Table 3 presents detailed information for the 10 hub nodes—*EPCAM, ALDH1A1* (aldehyde dehydrogenase 1 family member A1), *ZWINT, BUB1B* (BUB1 mitotic checkpoint serine/threonine kinase B), *NEK2* (NIMA-related kinase 2), *DLGAP5, MELK* (maternal embryonic leucine zipper kinase), *CEP55* (centrosomal protein 55), *CKS2* (CDC28 protein kinase regulatory subunit 2), and *KDR*. Among these hub genes, only *ALDH1A1* and *KDR* were downregulated.

Next, we performed module analysis in the MCODE app from Cytoscape to detect significant protein complexes

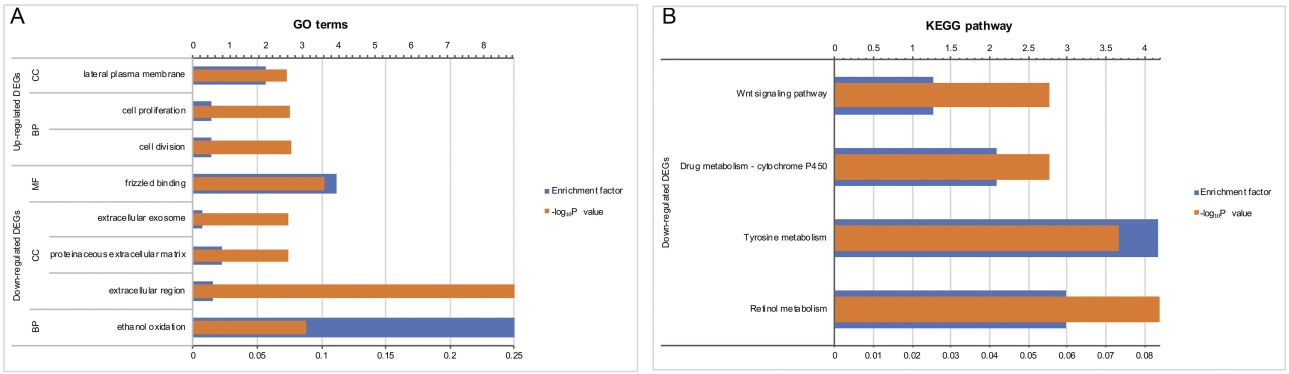

Figure 4 Functional enrichment analysis of the 103 integrated DEGs. (**A**) GO annotation. The *y*-axis shows significantly enriched GO terms, and the *x*-axis shows the enrichment factor and -$\log_{10}P$ values. (**B**) KEGG pathway enrichment analysis. The *y*-axis shows significantly enriched KEGG pathways, and the *x*-axis shows the enrichment factor and -$\log_{10}P$ values.

Note: The enrichment factor refers to the ratio of the number of DEGs enriched in a GO term/KEGG pathway to the total number of annotated genes enriched in the GO term/KEGG pathway.

Abbreviations: DEGs, differentially expressed genes; GO, Gene Ontology; KEGG, Kyoto Encyclopedia of Genes and Genomes; BP, biological process; CC, cellular component; MF, molecular function.

in this PPI network and obtained four modules (Figure 5B-E, Supplementary Table 8). Seven of the selected hub nodes were contained in module 1, suggesting that this module might play a key role in this PPI network. Thus, we performed further GO and KEGG enrichment analyses for module 1 (Supplementary Tables 9 and 10). As shown in Figure 6A, module 1 was closely correlated with a variety of GO terms, such as cell division, cell proliferation and mitotic nuclear division in the BP category; kinetochore and condensed chromosome kinetochore in the CC category; and protein binding in the MF category. The KEGG pathways enriched by the genes in module 1 included cell cycle and DNA replication (Figure 6B).

Survival Analysis

To explore the association between the aforementioned potential target genes and survival, the OS rates were calculated with the Kaplan-Meier Plotter website. A total of 1144 HGSOC patients from 9 datasets (TCGA, GSE9891, GSE26193, GSE63885, GSE18520, GSE30161, GSE14764, GSE23554 and GSE15622) were included in the OS analysis. Patients were stratified by low and high expression of each gene based on the best cutoff value. In the survival analysis (Supplementary Table 11), the expression levels of MELK, CEP55 and KDR were significantly correlated with the OS rates of patients with HGSOC ($P < 0.05$). Additionally, OS analyses of prespecified subgroups based on stage, grade, TP53 mutation and treatment were also performed (Supplementary Table 12). As shown in Figure 7A–C, a high MELK expression level was associated with a high OS rate for HGSOC patients, especially for those with advanced-stage disease (stages 3 and 4), grade 3 disease, and TP53 mutations and those administered platinum-containing chemotherapy regimens. High CEP55 expression afforded a poor OS, particularly for HGSOC patients in stage 3, without a TP53 mutation and treated with chemotherapy containing Taxol. Similarly, elevated KDR expression was significantly associated with a poor prognosis for HGSOC patients with grade 2 disease or under chemotherapy with Taxol ± platinum. Taken together, these findings indicate that MELK, CEP55 and KDR might represent important prognostic factors of survival for patients with HGSOC.

Validation Of Key Genes

Oncomine was used to analyze the expression of the ten selected hub genes in ovarian serous adenocarcinoma and normal ovarian tissues[35–38] (Table 4 and Figure 8). Our findings regarding the expression of the ten selected genes were consistent with the expression data in the Oncomine datasets; $P < 0.05$ indicated statistical significance. Specifically, EPCAM, ZWINT, BUB1B, NEK2, DLGAP5, MELK, CEP55 and CKS2 were upregulated, and ALDH1A1 and KDR were downregulated.

We performed qRT-PCR experiments to validate the expression of these ten hub genes in 22 HGSOC samples and 22 normal tissues. Consistent with the Oncomine data, the mRNA expression of *EPCAM, ZWINT, BUB1B, NEK2, DLGAP5, MELK*, and *CKS2* was significantly higher in HGSOC than in normal ovarian tissue, and the mRNA expression of *ALDH1A1* and *KDR* was lower in HGSOC tissues, as mentioned

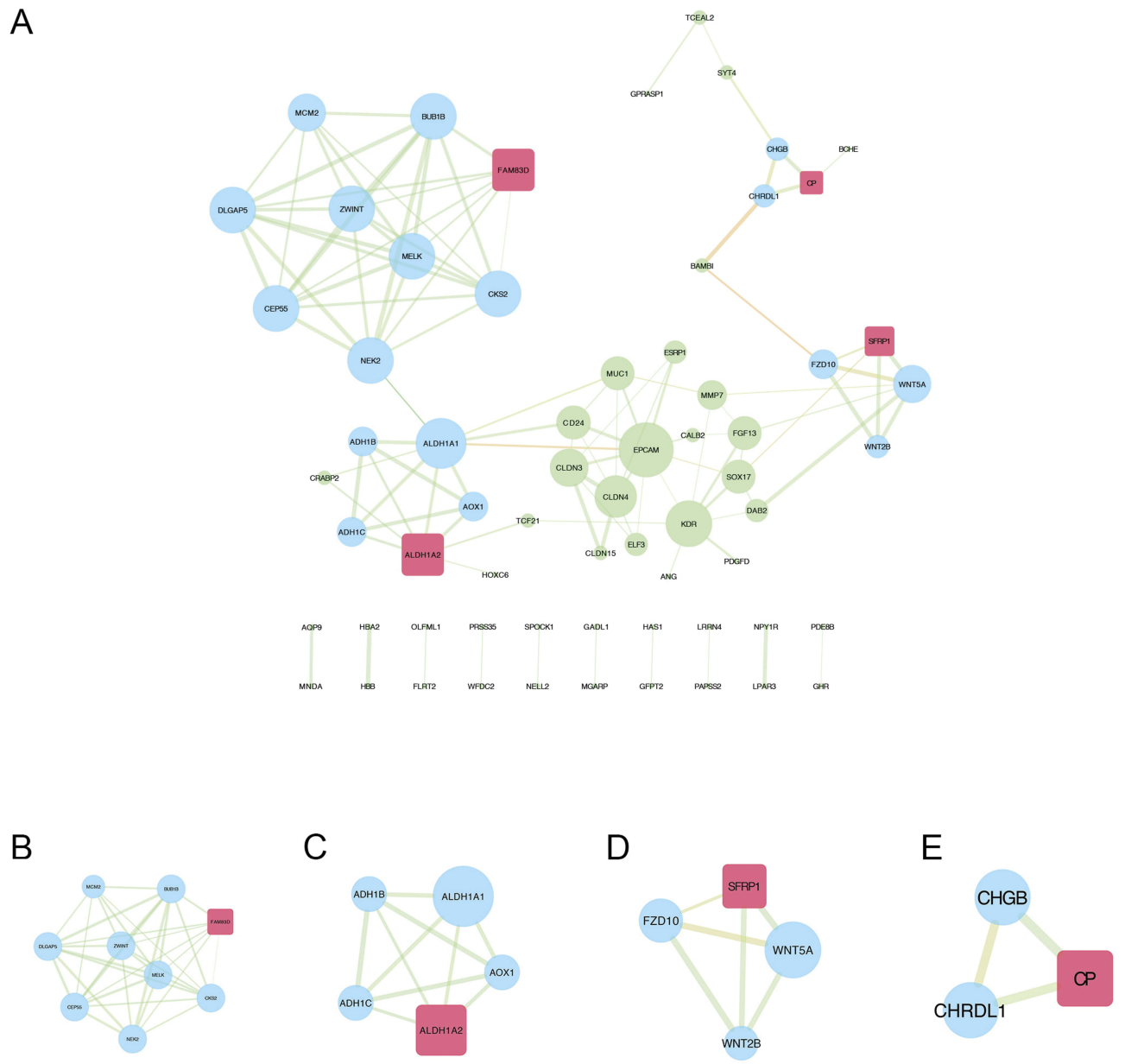

Figure 5 PPI network construction and module analysis of DEGs associated with HGSOC. (A) PPI network of the integrated DEGs visualized by Cytoscape software. The node size represents the node degree (a larger node indicates a higher degree). The width of the edge indicates the combined score (a wider edge indicates a higher combined score). The color of the edge represents the EdgeBetweenness (a more orange edge indicates a higher EdgeBetweenness). (B-E) MCODE module screening for the DEGs, including module 1 (MCODE score = 7, nodes = 9, edges = 69), module 2 (MCODE score = 4, nodes = 5, edges = 28), module 3 (MCODE score = 3, nodes = 4, edges = 17), and module 4 (MCODE score = 2, nodes = 3, edges = 9). The red rectangle indicates the seed gene, and the blue circles indicate the clustered genes.
Abbreviations: PPI, protein–protein interaction; DEGs, differentially expressed genes; HGSOC, high-grade serous ovarian cancer; MCODE, Molecular Complex Detection.

above (Figure 9). Although the mRNA expression level of CEP55 was elevated in HGSOC tissues compared with normal tissues, the difference was not statistically significant (Figure 9).

Additionally, we investigated EPCAM, ZWINT, DLGAP5, and KDR protein expression in clinical tissue specimens collected from patients. As shown in Figure 10, Western blotting confirmed the overexpression of both EPCAM and ZWINT and the downregulation of KDR in HGSOC tissues (n= 22) compared with normal ovarian tissues (n= 22). These results were consistent with the qRT-PCR results. However, DLGAP5 expression levels were not as expected. Although it is possible that complex physiological regulatory mechanisms lead to discrepant protein and RNA levels, more clinical samples are needed to verify the results for this gene.

Table 3 Information On The Ten Hub Nodes

Gene Name	Node Degree	Betweenness Centrality	Closeness Centrality	Category
EPCAM	10	0.36360281	0.34645669	Upregulated gene
ALDH1A1	9	0.47501762	0.32592593	Downregulated gene
ZWINT	8	0.00669486	0.22335025	Upregulated gene
BUB1B	8	0.00669486	0.22335025	Upregulated gene
NEK2	8	0.30443975	0.27160494	Upregulated gene
DLGAP5	8	0.00669486	0.22335025	Upregulated gene
MELK	8	0.00669486	0.22335025	Upregulated gene
CEP55	8	0.00669486	0.22335025	Upregulated gene
CKS2	8	0.00669486	0.22335025	Upregulated gene
KDR	8	0.16213254	0.30985915	Downregulated gene

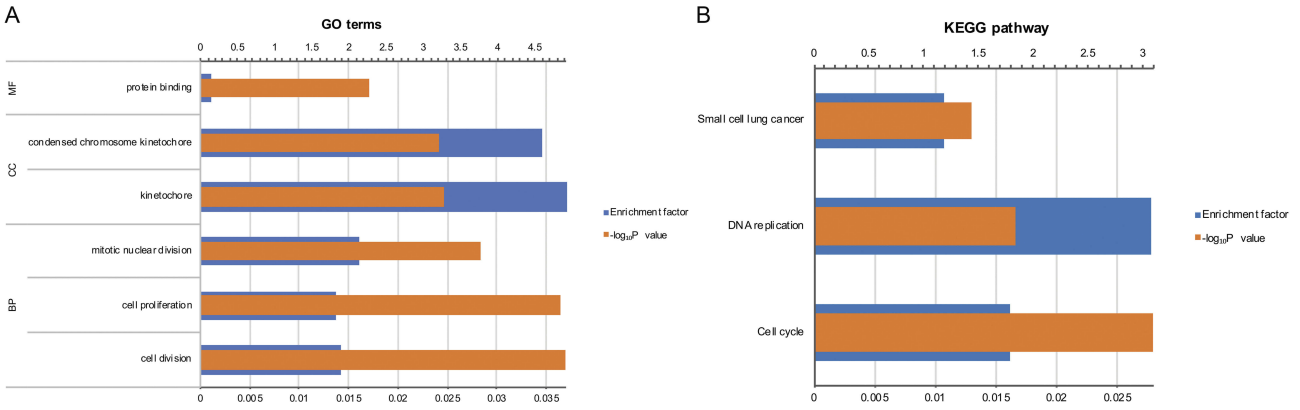

Figure 6 Functional enrichment analysis of the genes partitioned into module 1. (**A**) GO annotation. The *y*-axis shows significantly enriched GO terms, and the *x*-axis shows the enrichment factor and -$\log_{10}P$ values. (**B**) KEGG pathway enrichment analysis. The *y*-axis shows significantly enriched KEGG pathways, and the *x*-axis shows the enrichment factor and -$\log_{10}P$ values.
Abbreviations: GO, Gene Ontology; KEGG, Kyoto Encyclopedia of Genes and Genomes; BP, biological process; CC, cellular component; MF, molecular function.

Discussion

EOC is a highly lethal malignancy due to the difficulty of early diagnosis and the lack of effective treatments for advanced-stage disease. HGSOC, the main type of EOC, accounts for the majority of deaths. Therefore, it is essential to identify key genes associated with the early diagnosis and prognosis of HGSOC to improve the survival rate. Recently, integrated bioinformatics approaches based on microarray technology have been widely used to discover promising biomarkers for cancer diagnosis, treatment and prognosis.

In this study, we identified candidate biomarkers for HGSOC via integrated bioinformatic analysis. Six microarray datasets from GEO were integrated, and 103 DEGs between HGSOC and normal OSE samples were successfully identified, comprising 28 upregulated and 75 downregulated genes. Functional enrichment analysis showed that the upregulated genes were enriched in cell division and cell proliferation, which are critical for tumor growth, and that the downregulated genes mainly participated in various metabolic processes, including retinol metabolism, tyrosine metabolism, and drug metabolism/cytochrome P450 pathways, as well as the Wnt signaling pathway, which contributes to carcinogenesis.[40–42] A large number of studies have proposed that disorders in metabolism, including retinol metabolism[43,44] and tyrosine metabolism,[45,46] play important roles in carcinogenesis.

PPI network analysis enabled screening of the top 10 hub nodes according to the degree of connectivity, revealing eight upregulated genes (*EPCAM, ZWINT, BUB1B, NEK2, DLGAP5, MELK, CEP55* and *CKS2*) and two downregulated genes (*ALDH1A1* and *KDR*) that might be important in HGSOC pathogenesis. These ten genes can be used in the early diagnosis of patients with HGSOC. The expression levels of these ten hub genes were validated in five Oncomine datasets. In addition, we performed module analysis by using the MCODE app. Seven of the selected hub nodes, namely, *ZWINT,*

A. MELK

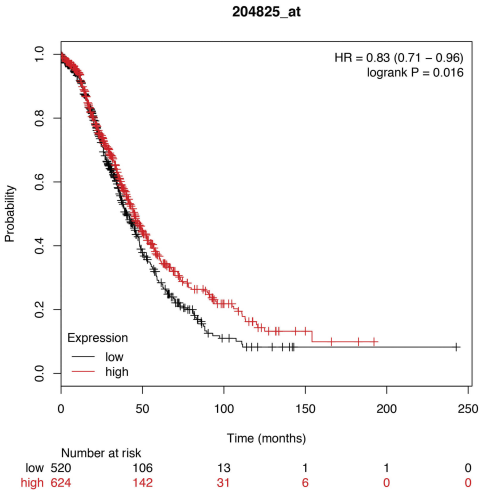

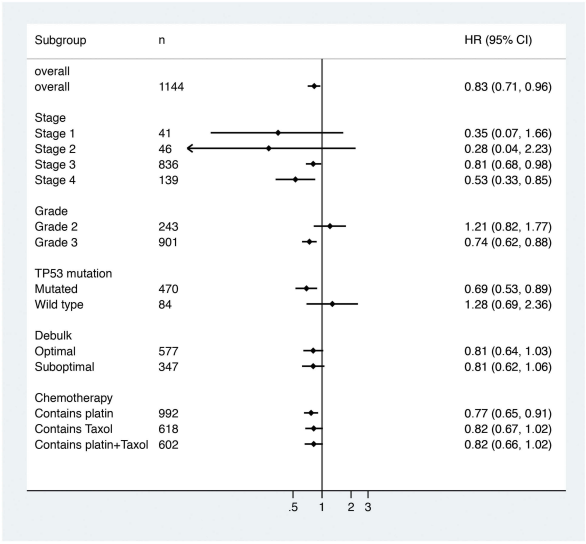

B. CEP55

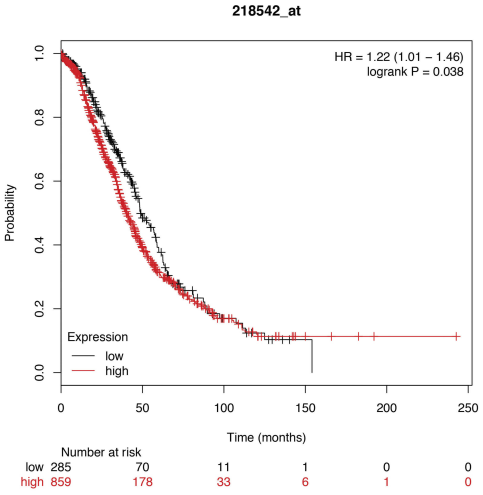

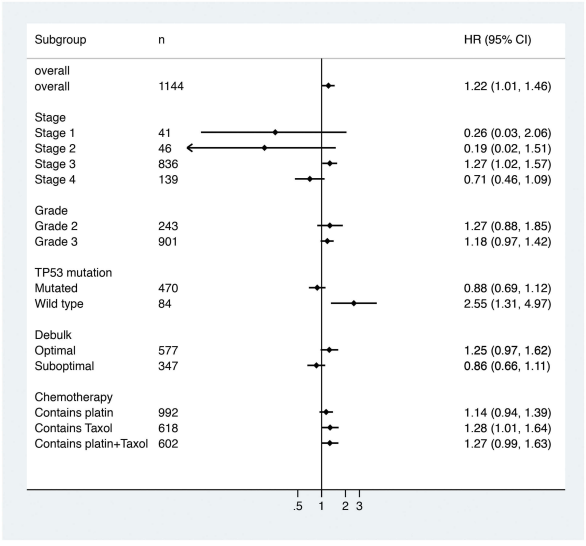

C. KDR

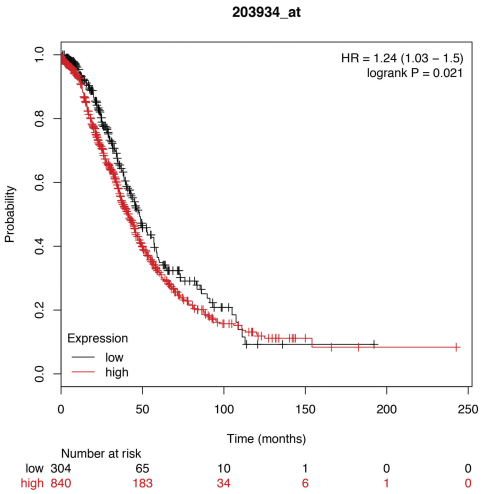

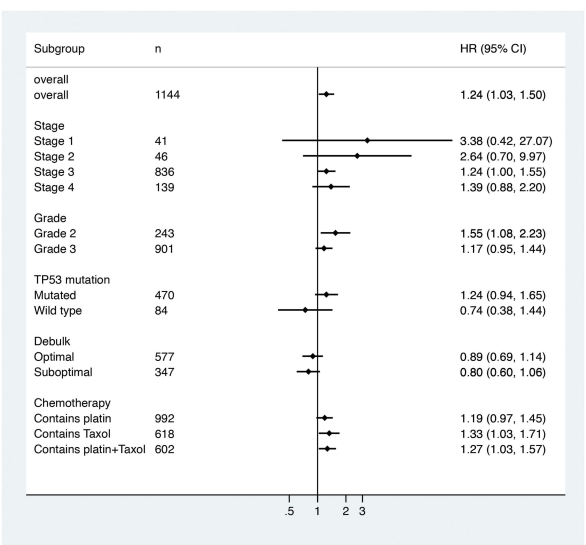

Figure 7 Survival curves and subgroup analyses of the OS rates of patients with HGSOC stratified by high and low expression of MELK (**A**), CEP55 (**B**) and KDR (**C**).
Abbreviations: OS, overall survival; HGSOC, high-grade serous ovarian cancer.

Table 4 Expression Of The Ten Selected Hub Genes In Five Oncomine Datasets

Gene Name	Welsh Ovarian, 2001[35]		Lu Ovarian, 2004[36]		Adib Ovarian, 2004[37]		Hendrix Ovarian, 2006[38]		TCGA Ovarian, 2013[39]	
	Fold Change	*P*-value	Fold Change	*P*-value	Fold Change	*P*-value	Fold Change	*P*-value	Fold Change	*P*-value
EPCAM	7.389	2.61E−09	7.44	4.25E−04	14.692	6.86E−05	2.867	4.44E−04	1.365	2.43E−04
ALDH1A1	−6.913	6.46E−12	−5.273	2.46E−04	−6.999	5.31E−04	−2.523	8.75E−13	−11.737	8.41E−08
ZWINT	NA	NA	2.662	1.61E−07	6.237	7.54E−04	1.541	9.37E−04	7.001	1.71E−05
BUB1B	NA	NA	2.312	3.07E−06	3.208	2.00E−03	1.514	2.20E−02	8.04	2.56E−07
NEK2	1.95	2.37E−06	1.186	1.10E−02	1.221	2.70E−02	1.22	3.05E−04	5.887	1.63E−06
DLGAP5	12.717	4.80E−02	1.321	2.00E−03	1.76	3.00E−03	1.479	3.70E−02	8.151	1.01E−06
MELK	23.125	1.90E−02	1.379	1.19E−04	1.331	5.05E−04	1.609	9.00E−03	10.6	2.98E−07
CEP55	NA	NA	2.457	9.44E−07	NA	NA	1.748	1.20E−02	8.075	1.50E−08
CKS2	13.417	4.20E−02	3.046	3.02E−08	4.612	8.00E−03	1.451	1.00E−02	5.956	3.85E−05
KDR	1.074	1.00E+00	−1.622	7.00E−03	−1.406	1.50E−02	−1.137	3.30E−02	−1.708	2.00E−03

Abbreviations: TCGA, the cancer genome atlas; NA, not available.

BUB1B, NEK2, DLGAP5, MELK, CEP55 and *CKS2*, partitioned into module 1; coincidentally, these nodes contained genes upregulated in HGSOC that are closely associated with cell cycle and DNA replication.

Survival analysis revealed that MELK, CEP55 and KDR expression levels were significantly correlated with the OS rates of patients with HGSOC. MELK overexpression was associated with prolonged OS for HGSOC patients, whereas increased CEP55 and KDR expression levels in HGSOC tissues were significantly associated with decreased OS rates for patients with HGSOC. Similar results were found in some prespecified subgroup analyses restricted to patients at different stages or grades or based on TP53 mutations and chemotherapy regimens. These analyses indicated that MELK, CEP55 and KDR are potential predictors of HGSOC prognosis.

Integrated bioinformatics methods are efficient tools for discovering promising biomarkers for cancer diagnosis, treatment and prognosis. However, further biological experiments are needed to validate these data analysis results. In this study, the significant expression levels of nine hub genes, namely, *EPCAM, ALDH1A1, ZWINT, BUB1B, NEK2, DLGAP5, MELK, CKS2* and *KDR*, were confirmed by qRT-PCR at the RNA level. The Western blotting experiments showed that EPCAM, ZWINT, and KDR protein expression levels were consistent with the database information; only the DLGAP5 expression level seemed contrary to expectations. Overall, our experimental results verified the reliability of this research approach.

The current study identified ten hub genes that might play important roles in HGSOC pathogenesis, and three hub genes were significantly associated with HGSOC prognosis. These genes have been widely studied in many other types of cancer.

MELK is a serine/threonine kinase in the Snf1 (sucrose nonfermenting 1)/AMPK family of kinases.[47] Multiple studies have reported that MELK is overexpressed and plays vital roles in various cancer types, including ovarian cancer,[48] colorectal cancer,[49] breast cancer,[50,51] small cell lung cancer,[52] brain cancer,[53] pancreatic cancer,[54] prostate cancer,[55] gastric cancer,[56,57] hepatocellular carcinoma,[58] and melanoma.[59] Pitner et al discussed the roles of MELK in cancer, including its ability to mediate proliferation, apoptosis, cancer stem cell phenotypes, epithelial-to-mesenchymal transition (EMT), metastasis, and therapeutic resistance, characterizing MELK as a promising therapeutic target.[60] In addition, Kohler et al showed that MELK overexpression was associated with histological grade ($P < 0.05$) and

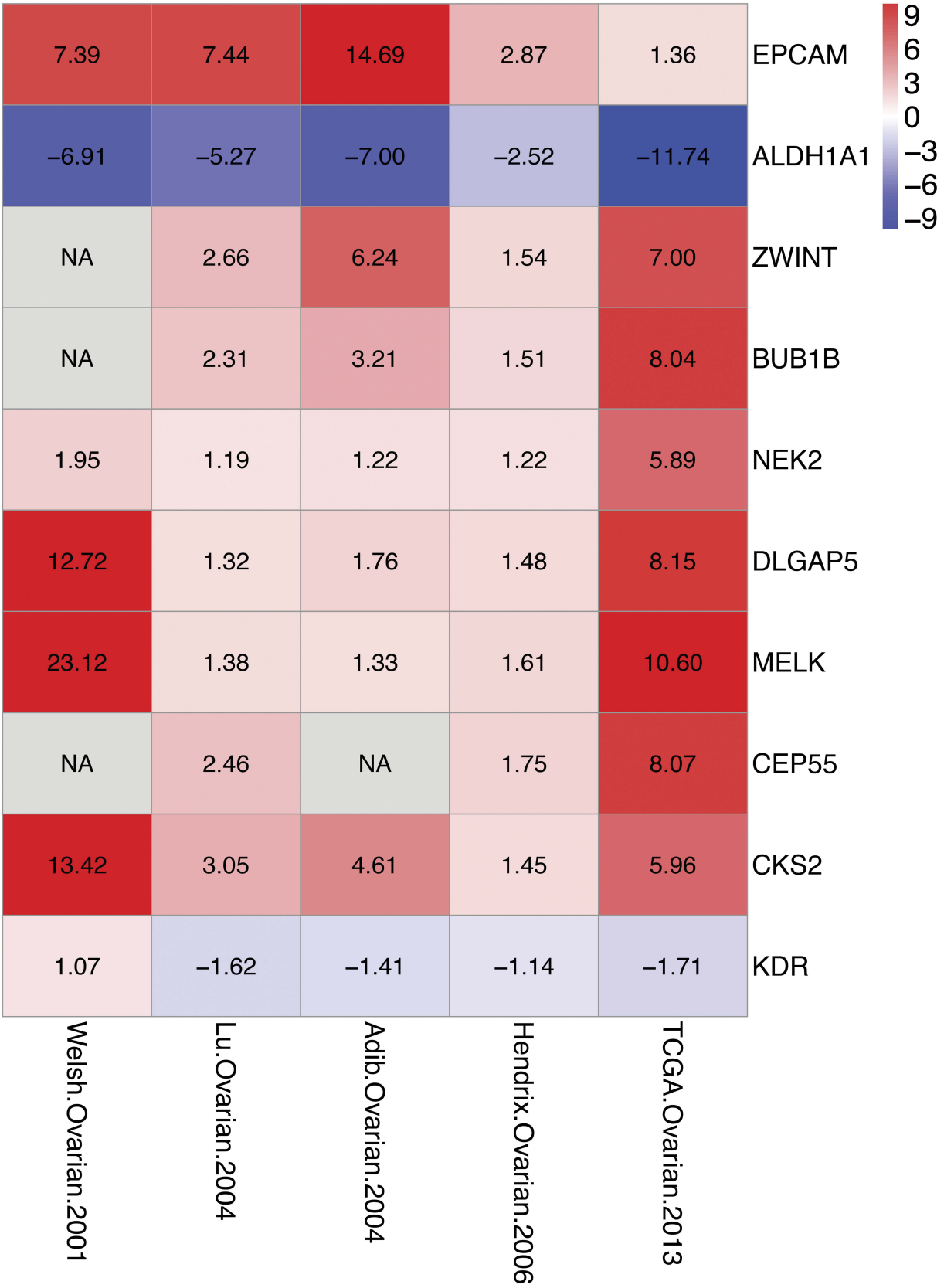

Figure 8 Heat map of the ten hub genes in the Oncomine datasets. Each column represents one dataset and each row represents one gene. The number in each rectangle is the log_2FC value. The color gradient from blue to red represents the progression from down- to upregulation.
Abbreviation: FC, fold change.

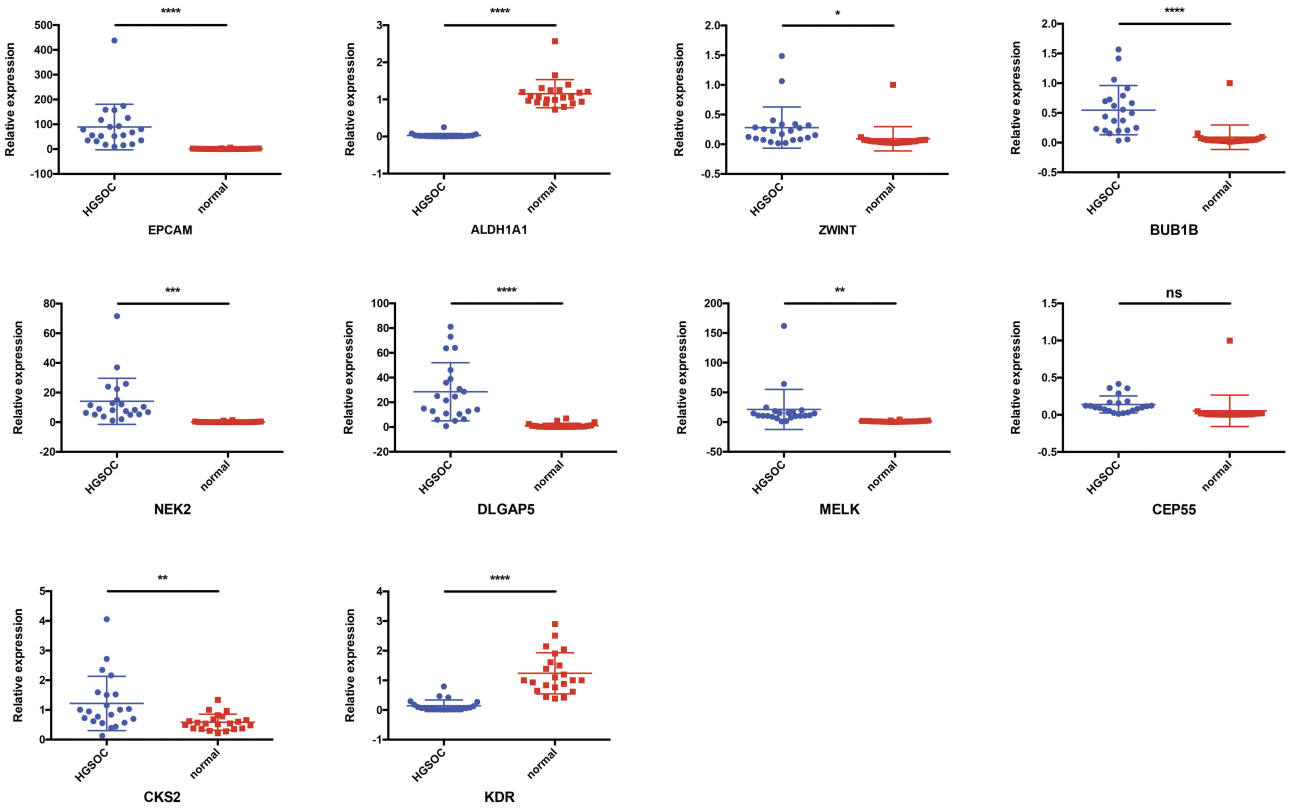

Figure 9 qRT-PCR analysis of the ten hub genes in 22 HGSOC and 22 normal ovarian samples. *P < 0.05, **P < 0.01, ***P < 0.001 and ****P < 0.0001.
Abbreviations: qRT-PCR, quantitative real-time PCR; HGSOC, high-grade serous ovarian cancer.

progression-free survival (HR = 5.73, P < 0.01) in patients with ovarian cancer;[48] notably, MELK was shown to participate in cell proliferation and tumor growth via cell cycle arrest at the G_2-M phase.[48] Gray et al reported the same results.[49] Multiple studies have reported that MELK overexpression in patients with cancer is correlated not only with poor prognosis[50,53,58] but also with chemoresistance and radioresistance.[61,62] Based on the above findings, MELK inhibition may be a novel strategy for the treatment aggressive malignancies and combining future MELK inhibitors with chemotherapy and/or radiotherapy may enhance the therapeutic effect of these traditional approaches.

Jeffery et al comprehensively discussed the roles of CEP55 in regulating the PI3K/AKT pathway and stemness and in promoting tumorigenesis.[63] CEP55 overexpression is common in cancer tissues and is correlated with an unfavorable prognosis in many human cancers, including non-small cell lung carcinoma,[64] pancreatic cancer,[65] osteosarcoma,[66] and ER+ breast cancer.[67] Shiraishi et al identified CEP55 as a marker to differentiate patients with prostate cancer recurrence following radical prostatectomy.[68] Tao et al discovered that CEP55 expression was strongly elevated in gastric cancer and that CEP55 overexpression promoted the proliferation, colony formation and tumorigenesis of gastric cancer cells.[69]

KDR, one of the two VEGF receptors, is also known as vascular endothelial growth factor receptor 2. It plays an essential role in regulating VEGF-induced endothelial proliferation, migration and sprouting and thus promoting angiogenesis, which is essential for cancer growth and metastasis. Takahashi et al showed that VEGF and KDR were overexpressed in metastatic colon cancer, which correlated with the vascularity, metastasis, and proliferation of human colon cancer.[70] An et al found that KDR mRNA expression levels were significantly higher in normal tissues than in lung cancer tissues. In addition, higher KDR expression levels in lung cancer tissues were associated with a shorter survival.[71] The prognostic value of KDR was also identified in patients with stage I non-small cell lung cancer.[72] The authors suggested that patients with KDR-positive tumors have a poor prognosis. Many studies have also reported that SNPs in KDR are associated with survival in patients with colorectal cancer.[73–75]

EPCAM is an epithelium-specific intercellular adhesion molecule that mediates Ca^{2+}-independent homophilic

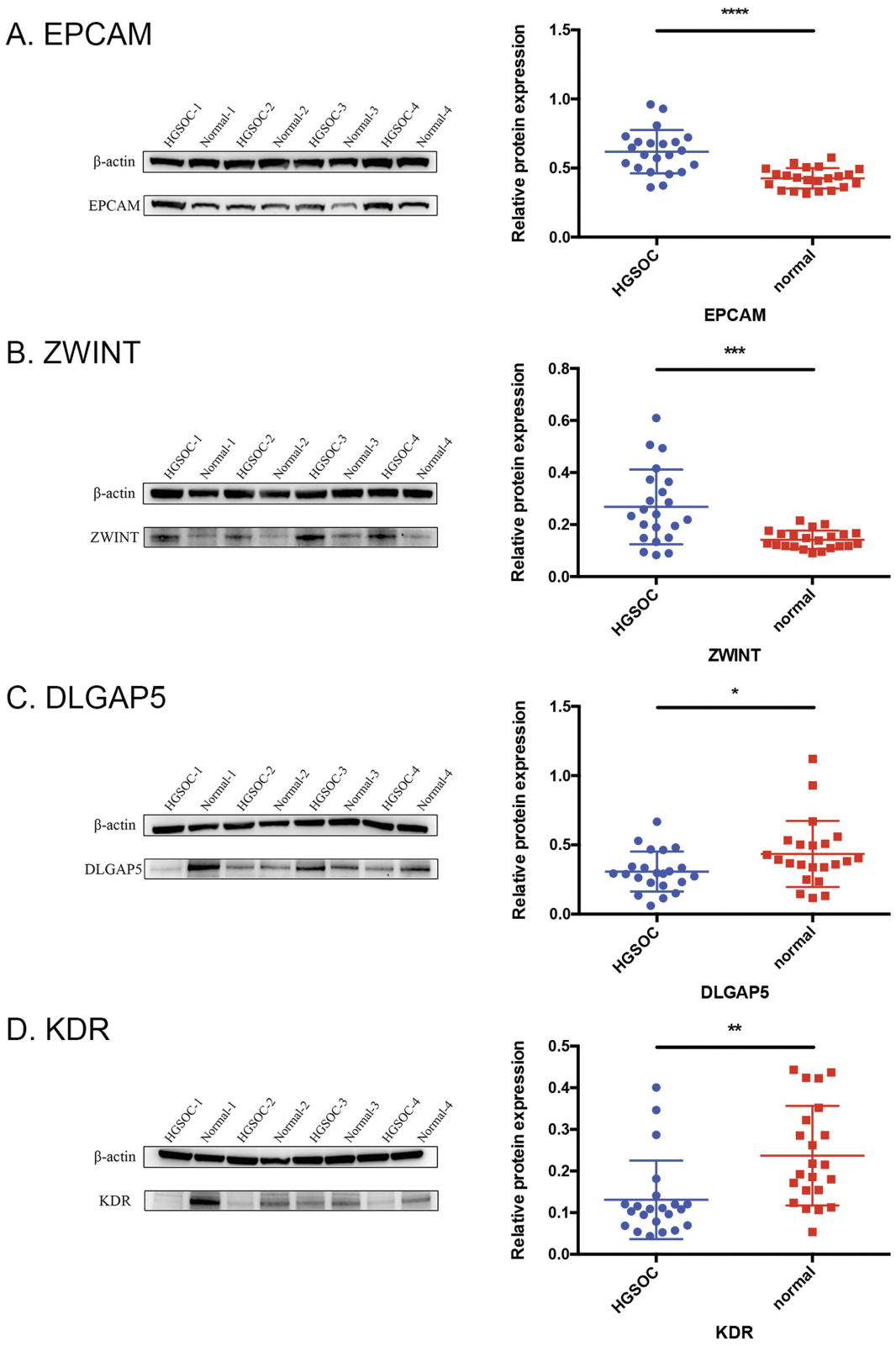

Figure 10 The protein expression levels of EPCAM (**A**), ZWINT (**B**), DLGAP5 (**C**) and KDR (**D**) in 22 HGSOC and 22 normal ovarian samples were analyzed by Western blotting. Signal intensities were quantified by ImageJ and normalized to an internal control (β-actin). *$P < 0.05$, **$P < 0.01$, ***$P < 0.001$ and ****$P < 0.0001$.
Abbreviation: HGSOC, high-grade serous ovarian cancer.

cell-cell adhesion.[76] EPCAM has been widely studied as a therapeutic target and a prognostic marker in various epithelial malignancies, including breast, ovarian, urothelial, and non-small cell lung carcinomas. Tayama et al found that high EPCAM levels correlated with chemotherapy resistance and poor prognosis in ovarian cancer patients; thus, targeting EPCAM is a potential promising approach to treat chemoresistant ovarian cancer.[77] However, data from Woopen et al showed that EPCAM overexpression in EOC was significantly associated with improved OS (P = 0.015) and an increased rate of response to platinum-based chemotherapy (P = 0.048).[78] Therefore, future large-scale and well-designed studies are warranted to validate these contradictory findings. In addition, Tomita et al demonstrated that EPCAM gene deletion attributed to Lynch syndrome (also known as hereditary nonpolyposis colorectal cancer, HNPCC) with MSH2 defects.[79] Notably, women with Lynch syndrome have a high risk of ovarian cancer. Liu et al reported that elevated EPCAM expression is correlated with metastasis and cell adhesion in breast cancer tissue.[80] In addition to being observed in epithelial malignancies, EPCAM overexpression is associated with larger tumor size, lymph node metastasis and a poorer prognosis in gastric cancer.[81] However, Wen et al provided evidence strengthening the role of EPCAM in endometrial carcinoma progression and prognosis and reported that EPCAM overexpression favored survival.[82] Furthermore, EPCAM was found to regulate EMT, which is important for cancer metastasis.[83,84]

The ZWINT protein is involved in kinetochore function and cell proliferation and is thought to be an important regulatory protein for chromosome movement and mitotic spindle checkpoints.[85,86] Consistent with our results, Xu et al identified ZWINT overexpression in ovarian cancer by integrated bioinformatic analysis and reported its association with reduced patient OS.[87] Urbanucci et al demonstrated that ZWINT expression was increased in patients with castration-resistant prostate cancer.[88] Moreover, ZWINT expression has been proven to be significantly upregulated and associated with tumor progression and poor prognosis in various cancers, including hepatocellular carcinoma[86] and lung cancer.[85] In contrast, a study by Yang et al indicated that ZWINT expression is downregulated in hepatocellular carcinoma and that patients with low ZWINT expression have a shorter OS and time to recurrence than patients with high ZWINT expression.[89] Further studies are required to define the detailed roles of ZWINT in cancer.

NEK2 is a centrosomal serine/threonine kinase that plays a critical regulatory role in mitosis. Recent studies have shown pivotal roles of NEK2 in the development of several cancers. Wu et al showed that NEK2 overexpression promoted liver cancer cell growth, metastasis and angiogenesis.[90] NEK2 induced chemotherapeutic resistance in patients with multiple myeloma,[91] hepatocellular carcinoma,[92] and nasopharyngeal carcinoma.[93] Many other reports have shown that high NEK2 expression predicts poor prognosis in various cancer types.[94–97]

DLGAP5, also known as HURP and DLG7 (disks large homolog 7), is a cell cycle-related protein that controls microtubule organization and is required for formation of the bipolar spindle.[98,99] Chen et al identified DLGAP5 as the direct target gene of NOTCH3 in ovarian cancer progression.[100] Many studies have suggested that DLGAP5 overexpression plays a role in carcinogenesis,[101] for example, in prostate cancer,[102] lung cancer,[103] gastric cancer,[104] pancreatic carcinoma,[105] and hepatocellular carcinoma.[106] Moreover, elevated DLGAP5 expression levels were strongly associated with poor survival in patients with non-small cell lung cancer,[107,108] breast cancer,[109] and adrenocortical carcinoma.[110] Moreover, Gomez et al found that DLGAP5 was significantly overexpressed in prostate cancer and that higher DLGAP5 transcript levels were associated with advanced tumor progression and worse prognosis in this disease.[111] Thus, DLGAP5 might be a novel biomarker of tumor progression and prognosis, but additional studies are needed to clarify its role in cancer.

CKS2, a cyclin-dependent kinase-interacting protein, is also a cell cycle regulatory protein. Studies have demonstrated that CKS2 expression is elevated in multiple types of cancer, including gastric cancer,[112,113] prostate cancer,[114] cholangiocarcinoma,[115] esophageal carcinoma,[116] and liver cancer.[117] CKS2 overexpression contributes to tumor progression and predicts an unfavorable prognosis. Kita et al found that CKS2 protein expression was significantly correlated with several clinicopathologic parameters, including the depth of tumor invasion, clinical stage and poor five-year survival in esophageal squamous cell carcinoma.[118] Yu et al reported that CKS2 was upregulated in colorectal cancer tissues and that CKS2 expression levels were significantly associated with tumor size and tumor stage. The author and his colleagues also observed that higher CKS2 expression predicted a poor outcome.[119]

Conclusion

In conclusion, by performing an integrated bioinformatic analysis of six GEO datasets, we identified ten hub genes

that might be involved in HGSOC pathogenesis. Module analysis placed seven of the selected hub nodes in module 1, in which cell cycle and DNA replication were identified as the crucial pathways enriched by the hub genes. Additionally, survival analysis revealed that three hub genes are associated with the OS rate in patients with HGSOC. Taken together, our findings reveal that *MELK, CEP55* and *KDR* are potential biomarkers that could facilitate the early diagnosis and treatment of HGSOC and predict the prognosis of patients with HGSOC. However, further molecular biology experiments are needed to verify our findings and confirm the potential clinical value of these genes as biomarkers.

Acknowledgments

This research was funded by the Chinese Academy of Medical Sciences Initiative for Innovative Medicine, grant number CAMS-2017-I2M-1-002.

Disclosure

The authors report no conflicts of interest in this work.

References

1. Siegel RL, Miller KD, Jemal A. Cancer statistics, 2018. *CA Cancer J Clin*. 2018;68(1):7–30. doi:10.3322/caac.21442
2. Howlader NNA, Krapcho M, Miller D, et al., editors. *SEER Cancer Statistics Review, 1975–2014, Based on November 2016 SEER Data Submission, Posted to the SEER Web Site, April 2017*. Bethesda, MD: National Cancer Institute; April 2017.
3. Prat J, Oncology F. Staging classification for cancer of the ovary, fallopian tube, and peritoneum. *Int J Gynaecol Obstet*. 2014;124 (1):1–5. doi:10.1016/j.ijgo.2013.10.001
4. Torre LA, Trabert B, DeSantis CE, et al. Ovarian cancer statistics, 2018. *CA Cancer J Clin*. 2018;68(4):284–296. doi:10.3322/caac.21456
5. Prat J. New insights into ovarian cancer pathology. *Ann Oncol*. 2012;23 Suppl 10:x111–117. doi:10.1093/annonc/mds300
6. Jelovac D, Armstrong DK. Recent progress in the diagnosis and treatment of ovarian cancer. *CA Cancer J Clin*. 2011;61(3):183–203. doi:10.3322/caac.v61:3
7. Morgan RJ Jr, Armstrong DK, Alvarez RD, et al. Ovarian cancer, version 1.2016, NCCN clinical practice guidelines in oncology. *J Natl Compr Canc Netw*. 2016;14(9):1134–1163. doi:10.6004/jnccn.2016.0122
8. Kurman RJ. Origin and molecular pathogenesis of ovarian high-grade serous carcinoma. *Ann Oncol*. 2013;24 Suppl 10:x16–21. doi:10.1093/annonc/mdt463
9. Singh N, Gilks CB, Wilkinson N, McCluggage WG. Assignment of primary site in high-grade serous tubal, ovarian and peritoneal carcinoma: a proposal. *Histopathology*. 2014;65(2):149–154. doi:10.1111/his.2014.65.issue-2
10. Zeppernick F, Meinhold-Heerlein I. The new FIGO staging system for ovarian, fallopian tube, and primary peritoneal cancer. *Arch Gynecol Obstet*. 2014;290(5):839–842. doi:10.1007/s00404-014-3364-8
11. McCluggage WG. Morphological subtypes of ovarian carcinoma: a review with emphasis on new developments and pathogenesis. *Pathology*. 2011;43(5):420–432. doi:10.1097/PAT.0b013e328348a6e7
12. Vang R, Shih IM, Kurman RJ. Ovarian low-grade and high-grade serous carcinoma: pathogenesis, clinicopathologic and molecular biologic features, and diagnostic problems. *Adv Anat Pathol*. 2009;16(5):267–282. doi:10.1097/PAP.0b013e3181b4fffa
13. Malpica A, Deavers MT, Tornos C, et al. Interobserver and intraobserver variability of a two-tier system for grading ovarian serous carcinoma. *Am J Surg Pathol*. 2007;31(8):1168–1174. doi:10.1097/PAS.0b013e31803199b0
14. Smyth GK, Michaud J, Scott HS. Use of within-array replicate spots for assessing differential expression in microarray experiments. *Bioinformatics*. 2005;21(9):2067–2075. doi:10.1093/bioinformatics/bti270
15. Ritchie ME, Phipson B, Wu D, et al. limma powers differential expression analyses for RNA-sequencing and microarray studies. *Nucleic Acids Res*. 2015;43(7):e47. doi:10.1093/nar/gkv007
16. Kolde R, Laur S, Adler P, Vilo J. Robust rank aggregation for gene list integration and meta-analysis. *Bioinformatics*. 2012;28(4):573–580. doi:10.1093/bioinformatics/btr709
17. Huang da W, Sherman BT, Lempicki RA. Systematic and integrative analysis of large gene lists using DAVID bioinformatics resources. *Nat Protoc*. 2009;4(1):44–57. doi:10.1038/nprot.2008.211
18. Ashburner M, Ball CA, Blake JA, et al; The Gene Ontology Consortium. Gene ontology: tool for the unification of biology. *Nat Genet*. 2000;25(1):25–29. doi:10.1038/75556
19. Yu G, Wang LG, Han Y, He QY. clusterProfiler: an R package for comparing biological themes among gene clusters. *OMICS*. 2012;16(5):284–287. doi:10.1089/omi.2011.0118
20. Kanehisa M, Goto S, Furumichi M, Tanabe M, Hirakawa M. KEGG for representation and analysis of molecular networks involving diseases and drugs. *Nucleic Acids Res*. 2010;38(Database issue):D355–D360.
21. Benjamini Y, Hochberg Y. Controlling the false discovery rate - a practical and powerful approach to multiple testing. *J R Stat Soc B*. 1995;57(1):289–300.
22. Szklarczyk D, Morris JH, Cook H, et al. The STRING database in 2017: quality-controlled protein-protein association networks, made broadly accessible. *Nucleic Acids Res*. 2017;45(D1):D362–D368. doi:10.1093/nar/gkw937
23. Shannon P, Markiel A, Ozier O, et al. Cytoscape: a software environment for integrated models of biomolecular interaction networks. *Genome Res*. 2003;13(11):2498–2504. doi:10.1101/gr.1239303
24. Williams O, Del Genio CI. Degree correlations in directed scale-free networks. *PLoS One*. 2014;9(10):e110121. doi:10.1371/journal.pone.0110121
25. Bader GD, Hogue CW. An automated method for finding molecular complexes in large protein interaction networks. *BMC Bioinformatics*. 2003;4:2. doi:10.1186/1471-2105-4-2
26. Nagy A, Lanczky A, Menyhart O, Gyorffy B. Validation of miRNA prognostic power in hepatocellular carcinoma using expression data of independent datasets. *Sci Rep*. 2018;8(1):9227. doi:10.1038/s41598-018-27521-y
27. Gyorffy B, Lanczky A, Szallasi Z. Implementing an online tool for genome-wide validation of survival-associated biomarkers in ovarian-cancer using microarray data from 1287 patients. *Endocr Relat Cancer*. 2012;19(2):197–208. doi:10.1530/ERC-11-0329
28. Tung CS, Mok SC, Tsang YT, et al. PAX2 expression in low malignant potential ovarian tumors and low-grade ovarian serous carcinomas. *Mod Pathol*. 2009;22(9):1243–1250.
29. Mok SC, Bonome T, Vathipadiekal V, et al. A gene signature predictive for outcome in advanced ovarian cancer identifies a survival factor: microfibril-associated glycoprotein 2. *Cancer Cell*. 2009;16(6):521–532. doi:10.1016/j.ccr.2009.10.018
30. Bonome T, Levine DA, Shih J, et al. A gene signature predicting for survival in suboptimally debulked patients with ovarian cancer. *Cancer Res*. 2008;68(13):5478–5486. doi:10.1158/0008-5472.CAN-07-6595

31. Vathipadiekal V, Wang V, Wei W, et al. Creation of a human secretome: a novel composite library of human secreted proteins: validation using ovarian cancer gene expression data and a virtual secretome array. *Clin Cancer Res*. 2015;21(21):4960–4969. doi:10.1158/1078-0432.CCR-14-3173
32. King ER, Tung CS, Tsang YT, et al. The anterior gradient homolog 3 (AGR3) gene is associated with differentiation and survival in ovarian cancer. *Am J Surg Pathol*. 2011;35(6):904–912. doi:10.1097/PAS.0b013e318212ae22
33. Yeung TL, Leung CS, Wong KK, et al. TGF-beta modulates ovarian cancer invasion by upregulating CAF-derived versican in the tumor microenvironment. *Cancer Res*. 2013;73(16):5016–5028. doi:10.1158/0008-5472.CAN-13-0023
34. Yeung TL, Leung CS, Wong KK, et al. ELF3 is a negative regulator of epithelial-mesenchymal transition in ovarian cancer cells. *Oncotarget*. 2017;8(10):16951–16963. doi:10.18632/oncotarget.15208
35. Welsh JB, Zarrinkar PP, Sapinoso LM, et al. Analysis of gene expression profiles in normal and neoplastic ovarian tissue samples identifies candidate molecular markers of epithelial ovarian cancer. *Proc Natl Acad Sci U S A*. 2001;98(3):1176–1181. doi:10.1073/pnas.98.3.1176
36. Lu KH, Patterson AP, Wang L, et al. Selection of potential markers for epithelial ovarian cancer with gene expression arrays and recursive descent partition analysis. *Clin Cancer Res*. 2004;10(10):3291–3300. doi:10.1158/1078-0432.CCR-03-0409
37. Adib TR, Henderson S, Perrett C, et al. Predicting biomarkers for ovarian cancer using gene-expression microarrays. *Br J Cancer*. 2004;90(3):686–692. doi:10.1038/sj.bjc.6601603
38. Hendrix ND, Wu R, Kuick R, Schwartz DR, Fearon ER, Cho KR. Fibroblast growth factor 9 has oncogenic activity and is a downstream target of Wnt signaling in ovarian endometrioid adenocarcinomas. *Cancer Res*. 2006;66(3):1354–1362. doi:10.1158/0008-5472.CAN-05-3694
39. Verhaak RG, Tamayo P, Yang JY, et al. Prognostically relevant gene signatures of high-grade serous ovarian carcinoma. *J Clin Invest*. 2013;123(1):517–525.
40. Ford CE, Henry C, Llamosas E, Djordjevic A, Hacker N. Wnt signalling in gynaecological cancers: A future target for personalised medicine?. *Gynecol Oncol*. 2016;140(2):345–351. doi:10.1016/j.ygyno.2015.09.085
41. Zhan T, Rindtorff N, Boutros M. Wnt signaling in cancer. *Oncogene*. 2017;36(11):1461–1473. doi:10.1038/onc.2016.304
42. Losi L, Fonda S, Saponaro S, et al. Distinct DNA methylation profiles in ovarian tumors: opportunities for novel biomarkers. *Int J Mol Sci*. 2018;19(6). doi:10.3390/ijms19061559
43. Losi L, Lauriola A, Tazzioli E, et al. Involvement of epigenetic modification of TERT promoter in response to all-trans retinoic acid in ovarian cancer cell lines. *J Ovarian Res*. 2019;12(1):62. doi:10.1186/s13048-019-0536-y
44. Ni X, Hu G, Cai X. The success and the challenge of all-trans retinoic acid in the treatment of cancer. *Crit Rev Food Sci Nutr*. 2019;59(sup1):S71–S80. doi:10.1080/10408398.2018.1509201
45. Yu Y, Suryo Rahmanto Y, Lee MH, et al. Inhibition of ovarian tumor cell invasiveness by targeting SYK in the tyrosine kinase signaling pathway. *Oncogene*. 2018;37(28):3778–3789. doi:10.1038/s41388-018-0241-0
46. Jannin A, Penel N, Ladsous M, Vantyghem MC, Do Cao C. Tyrosine kinase inhibitors and immune checkpoint inhibitors-induced thyroid disorders. *Crit Rev Oncol Hematol*. 2019;141:23–35. doi:10.1016/j.critrevonc.2019.05.015
47. Heyer BS, Warsowe J, Solter D, Knowles BB, Ackerman SL. New member of the Snf1/AMPK kinase family, Melk, is expressed in the mouse egg and preimplantation embryo. *Mol Reprod Dev*. 1997;47(2):148–156. doi:10.1002/(ISSN)1098-2795
48. Kohler RS, Kettelhack H, Knipprath-Meszaros AM, et al. MELK expression in ovarian cancer correlates with poor outcome and its inhibition by OTSSP167 abrogates proliferation and viability of ovarian cancer cells. *Gynecol Oncol*. 2017;145(1):159–166. doi:10.1016/j.ygyno.2017.02.016
49. Gray D, Jubb AM, Hogue D, et al. Maternal embryonic leucine zipper kinase/murine protein serine-threonine kinase 38 is a promising therapeutic target for multiple cancers. *Cancer Res*. 2005;65(21):9751–9761. doi:10.1158/0008-5472.CAN-04-4531
50. Pickard MR, Green AR, Ellis IO, et al. Dysregulated expression of Fau and MELK is associated with poor prognosis in breast cancer. *Breast Cancer Res*. 2009;11(4):R60. doi:10.1186/bcr2350
51. Wang Y, Lee YM, Baitsch L, et al. MELK is an oncogenic kinase essential for mitotic progression in basal-like breast cancer cells. *Elife*. 2014;3:e01763. doi:10.7554/eLife.01763
52. Inoue H, Kato T, Olugbile S, et al. Effective growth-suppressive activity of maternal embryonic leucine-zipper kinase (MELK) inhibitor against small cell lung cancer. *Oncotarget*. 2016;7(12):13621–13633. doi:10.18632/oncotarget.v7i12
53. Nakano I, Masterman-Smith M, Saigusa K, et al. Maternal embryonic leucine zipper kinase is a key regulator of the proliferation of malignant brain tumors, including brain tumor stem cells. *J Neurosci Res*. 2008;86(1):48–60. doi:10.1002/jnr.v86:1
54. Ganguly R, Hong CS, Smith LG, Kornblum HI, Nakano I. Maternal embryonic leucine zipper kinase: key kinase for stem cell phenotype in glioma and other cancers. *Mol Cancer Ther*. 2014;13(6):1393–1398. doi:10.1158/1535-7163.MCT-13-0764
55. Kuner R, Falth M, Pressinotti NC, et al. The maternal embryonic leucine zipper kinase (MELK) is upregulated in high-grade prostate cancer. *J Mol Med (Berl)*. 2013;91(2):237–248. doi:10.1007/s00109-012-0949-1
56. Calcagno DQ, Takeno SS, Gigek CO, et al. Identification of IL11RA and MELK amplification in gastric cancer by comprehensive genomic profiling of gastric cancer cell lines. *World J Gastroenterol*. 2016;22(43):9506–9514. doi:10.3748/wjg.v22.i43.9506
57. Du T, Qu Y, Li J, et al. Maternal embryonic leucine zipper kinase enhances gastric cancer progression via the FAK/Paxillin pathway. *Mol Cancer*. 2014;13:100. doi:10.1186/1476-4598-13-100
58. Xia H, Kong SN, Chen J, et al. MELK is an oncogenic kinase essential for early hepatocellular carcinoma recurrence. *Cancer Lett*. 2016;383(1):85–93. doi:10.1016/j.canlet.2016.09.017
59. Janostiak R, Rauniyar N, Lam TT, et al. MELK promotes melanoma growth by stimulating the NF-kappaB pathway. *Cell Rep*. 2017;21(10):2829–2841. doi:10.1016/j.celrep.2017.11.033
60. Pitner MK, Taliaferro JM, Dalby KN, Bartholomeusz C. MELK: a potential novel therapeutic target for TNBC and other aggressive malignancies. *Expert Opin Ther Targets*. 2017;21(9):849–859. doi:10.1080/14728222.2017.1363183
61. Speers C, Zhao SG, Kothari V, et al. Maternal Embryonic Leucine Zipper Kinase (MELK) as a novel mediator and biomarker of radioresistance in human breast cancer. *Clin Cancer Res*. 2016;22(23):5864–5875. doi:10.1158/1078-0432.CCR-15-2711
62. Choi S, Ku JL. Resistance of colorectal cancer cells to radiation and 5-FU is associated with MELK expression. *Biochem Biophys Res Commun*. 2011;412(2):207–213. doi:10.1016/j.bbrc.2011.07.060
63. Jeffery J, Sinha D, Srihari S, Kalimutho M, Khanna KK. Beyond cytokinesis: the emerging roles of CEP55 in tumorigenesis. *Oncogene*. 2016;35(6):683–690. doi:10.1038/onc.2015.128
64. Jiang C, Zhang Y, Li Y, et al. High CEP55 expression is associated with poor prognosis in non-small-cell lung cancer. *Onco Targets Ther*. 2018;11:4979–4990. doi:10.2147/OTT
65. Peng T, Zhou W, Guo F, et al. Centrosomal protein 55 activates NF-kappaB signalling and promotes pancreatic cancer cells aggressiveness. *Sci Rep*. 2017;7(1):5925. doi:10.1038/s41598-017-06132-z

66. Xu L, Xia C, Sheng F, Sun Q, Xiong J, Wang S. CEP55 promotes the proliferation and invasion of tumour cells via the AKT signalling pathway in osteosarcoma. *Carcinogenesis*. 2018;39(4):623–631. doi:10.1093/carcin/bgy017
67. Martin KJ, Patrick DR, Bissell MJ, Fournier MV. Prognostic breast cancer signature identified from 3D culture model accurately predicts clinical outcome across independent datasets. *PLoS One*. 2008;3(8):e2994. doi:10.1371/journal.pone.0002994
68. Shiraishi T, Terada N, Zeng Y, et al. Cancer/Testis Antigens as potential predictors of biochemical recurrence of prostate cancer following radical prostatectomy. *J Transl Med*. 2011;9:153. doi:10.1186/1479-5876-9-153
69. Tao J, Zhi X, Tian Y, et al. CEP55 contributes to human gastric carcinoma by regulating cell proliferation. *Tumour Biol*. 2014;35(5):4389–4399. doi:10.1007/s13277-013-1578-1
70. Takahashi Y, Kitadai Y, Bucana CD, Cleary KR, Ellis LM. Expression of vascular endothelial growth factor and its receptor, KDR, correlates with vascularity, metastasis, and proliferation of human colon cancer. *Cancer Res*. 1995;55(18):3964–3968.
71. An SJ, Nie Q, Chen ZH, et al. KDR expression is associated with the stage and cigarette smoking of the patients with lung cancer. *J Cancer Res Clin Oncol*. 2007;133(9):635–642. doi:10.1007/s00432-007-0214-0
72. Seto T, Higashiyama M, Funai H, et al. Prognostic value of expression of vascular endothelial growth factor and its flt-1 and KDR receptors in stage I non-small-cell lung cancer. *Lung Cancer*. 2006;53(1):91–96. doi:10.1016/j.lungcan.2006.02.009
73. Slattery ML, Lundgreen A, Wolff RK. VEGFA, FLT1, KDR and colorectal cancer: assessment of disease risk, tumor molecular phenotype, and survival. *Mol Carcinog*. 2014;53 Suppl 1:E140–E150. doi:10.1002/mc.22058
74. Dong G, Guo X, Fu X, et al. Potentially functional genetic variants in KDR gene as prognostic markers in patients with resected colorectal cancer. *Cancer Sci*. 2012;103(3):561–568. doi:10.1111/j.1349-7006.2011.02194.x
75. Jang MJ, Jeon YJ, Kim JW, et al. Association of VEGF and KDR single nucleotide polymorphisms with colorectal cancer susceptibility in Koreans. *Mol Carcinog*. 2013;52 Suppl 1:E60–69. doi:10.1002/mc.21980
76. Litvinov SV, Velders MP, Bakker HA, Fleuren GJ, Warnaar SO. Ep-CAM: a human epithelial antigen is a homophilic cell-cell adhesion molecule. *J Cell Biol*. 1994;125(2):437–446. doi:10.1083/jcb.125.2.437
77. Tayama S, Motohara T, Narantuya D, et al. The impact of EpCAM expression on response to chemotherapy and clinical outcomes in patients with epithelial ovarian cancer. *Oncotarget*. 2017;8(27):44312–44325. doi:10.18632/oncotarget.v8i27
78. Woopen H, Pietzner K, Richter R, et al. Overexpression of the epithelial cell adhesion molecule is associated with a more favorable prognosis and response to platinum-based chemotherapy in ovarian cancer. *J Gynecol Oncol*. 2014;25(3):221–228. doi:10.3802/jgo.2014.25.3.221
79. Tomita N, Yamano T, Matsubara N, Tamura K. [A novel genetic disorder of Lynch syndrome - EPCAM gene deletion]. *Gan To Kagaku Ryoho*. 2013;40(2):143–147.
80. Liu X, Gao J, Sun Y, et al. Mutation of N-linked glycosylation in EpCAM affected cell adhesion in breast cancer cells. *Biol Chem*. 2017;398(10):1119–1126. doi:10.1515/hsz-2016-0232
81. Dai M, Yuan F, Fu C, Shen G, Hu S, Shen G. Relationship between epithelial cell adhesion molecule (EpCAM) overexpression and gastric cancer patients: a systematic review and meta-analysis. *PLoS One*. 2017;12(4):e0175357. doi:10.1371/journal.pone.0175357
82. Wen KC, Sung PL, Chou YT, et al. The role of EpCAM in tumor progression and the clinical prognosis of endometrial carcinoma. *Gynecol Oncol*. 2018;148(2):383–392. doi:10.1016/j.ygyno.2017.11.033
83. Sankpal NV, Fleming TP, Sharma PK, Wiedner HJ, Gillanders WE. A double-negative feedback loop between EpCAM and ERK contributes to the regulation of epithelial-mesenchymal transition in cancer. *Oncogene*. 2017;36(26):3706–3717. doi:10.1038/onc.2016.504
84. Hsu YT, Osmulski P, Wang Y, et al. EpCAM-regulated transcription exerts influences on nanomechanical properties of endometrial cancer cells that promote epithelial-to-mesenchymal transition. *Cancer Res*. 2016;76(21):6171–6182. doi:10.1158/0008-5472.CAN-16-0752
85. Peng F, Li Q, Niu SQ, et al. ZWINT is the next potential target for lung cancer therapy. *J Cancer Res Clin Oncol*. 2019;145:661–673. doi:10.1007/s00432-018-2823-1
86. Ying H, Xu Z, Chen M, Zhou S, Liang X, Cai X. Overexpression of Zwint predicts poor prognosis and promotes the proliferation of hepatocellular carcinoma by regulating cell-cycle-related proteins. *Onco Targets Ther*. 2018;11:689–702. doi:10.2147/OTT
87. Xu Z, Zhou Y, Cao Y, Dinh TL, Wan J, Zhao M. Identification of candidate biomarkers and analysis of prognostic values in ovarian cancer by integrated bioinformatics analysis. *Med Oncol*. 2016;33(11):130. doi:10.1007/s12032-016-0840-y
88. Urbanucci A, Sahu B, Seppala J, et al. Overexpression of androgen receptor enhances the binding of the receptor to the chromatin in prostate cancer. *Oncogene*. 2012;31(17):2153–2163. doi:10.1038/onc.2011.401
89. Yang XY, Wu B, Ma SL, Yin L, Wu MC, Li AJ. Decreased expression of ZWINT is associated with poor prognosis in patients with HCC after surgery. *Technol Cancer Res Treat*. 2018;17:1533033818794190. doi:10.1177/1533033818794190
90. Wu SM, Lin SL, Lee KY, et al. Hepatoma cell functions modulated by NEK2 are associated with liver cancer progression. *Int J Cancer*. 2017;140(7):1581–1596. doi:10.1002/ijc.30559
91. Zhou W, Yang Y, Xia J, et al. NEK2 induces drug resistance mainly through activation of efflux drug pumps and is associated with poor prognosis in myeloma and other cancers. *Cancer Cell*. 2013;23(1):48–62. doi:10.1016/j.ccr.2012.12.001
92. Lin S, Zhou S, Jiang S, et al. NEK2 regulates stem-like properties and predicts poor prognosis in hepatocellular carcinoma. *Oncol Rep*. 2016;36(2):853–862. doi:10.3892/or.2016.4896
93. Xu H, Zeng L, Guan Y, et al. High NEK2 confers to poor prognosis and contributes to cisplatin-based chemotherapy resistance in nasopharyngeal carcinoma. *J Cell Biochem*. 2019;120(3):3547–3558. doi:10.1002/jcb.v120.3
94. Neal CP, Fry AM, Moreman C, et al. Overexpression of the Nek2 kinase in colorectal cancer correlates with beta-catenin relocalization and shortened cancer-specific survival. *J Surg Oncol*. 2014;110(7):828–838. doi:10.1002/jso.v110.7
95. Li G, Zhong Y, Shen Q, et al. NEK2 serves as a prognostic biomarker for hepatocellular carcinoma. *Int J Oncol*. 2017;50(2):405–413. doi:10.3892/ijo.2017.3837
96. Liu H, Liu B, Hou X, et al. Overexpression of NIMA-related kinase 2 is associated with poor prognoses in malignant glioma. *J Neurooncol*. 2017;132(3):409–417. doi:10.1007/s11060-017-2401-4
97. Zhang Y, Wang W, Wang Y, et al. NEK2 promotes hepatocellular carcinoma migration and invasion through modulation of the epithelial-mesenchymal transition. *Oncol Rep*. 2018;39(3):1023–1033. doi:10.3892/or.2018.6224
98. Sillje HH, Nagel S, Korner R, Nigg EA. HURP is a Ran-importin beta-regulated protein that stabilizes kinetochore microtubules in the vicinity of chromosomes. *Curr Biol*. 2006;16(8):731–742. doi:10.1016/j.cub.2006.02.070
99. Koffa MD, Casanova CM, Santarella R, Kocher T, Wilm M, Mattaj IW. HURP is part of a Ran-dependent complex involved in spindle formation. *Curr Biol*. 2006;16(8):743–754. doi:10.1016/j.cub.2006.03.056
100. Chen X, Thiaville MM, Chen L, et al. Defining NOTCH3 target genes in ovarian cancer. *Cancer Res*. 2012;72(9):2294–2303. doi:10.1158/0008-5472.CAN-11-2181

101. Sanderson HS, Clarke PR. Cell biology: ran, mitosis and the cancer connection. *Curr Biol*. 2006;16(12):R466–468. doi:10.1016/j.cub.2006.05.032
102. Horning AM, Wang Y, Lin CK, et al. Single-cell RNA-seq reveals a subpopulation of prostate cancer cells with enhanced cell-cycle-related transcription and attenuated androgen response. *Cancer Res*. 2018;78(4):853–864. doi:10.1158/0008-5472.CAN-17-1924
103. Shi YX, Yin JY, Shen Y, Zhang W, Zhou HH, Liu ZQ. Genome-scale analysis identifies NEK2, DLGAP5 and ECT2 as promising diagnostic and prognostic biomarkers in human lung cancer. *Sci Rep*. 2017;7(1):8072. doi:10.1038/s41598-017-08615-5
104. Liu J, Liu Z, Zhang X, Gong T, Yao D. Examination of the expression and prognostic significance of DLGAPs in gastric cancer using the TCGA database and bioinformatic analysis. *Mol Med Rep*. 2018;18(6):5621–5629. doi:10.3892/mmr.2018.9574
105. Zhou Z, Cheng Y, Jiang Y, et al. Ten hub genes associated with progression and prognosis of pancreatic carcinoma identified by co-expression analysis. *Int J Biol Sci*. 2018;14(2):124–136. doi:10.7150/ijbs.22619
106. Liao W, Liu W, Yuan Q, et al. Silencing of DLGAP5 by siRNA significantly inhibits the proliferation and invasion of hepatocellular carcinoma cells. *PLoS One*. 2013;8(12):e80789. doi:10.1371/journal.pone.0080789
107. Schneider MA, Christopoulos P, Muley T, et al. AURKA, DLGAP5, TPX2, KIF11 and CKAP5: five specific mitosis-associated genes correlate with poor prognosis for non-small cell lung cancer patients. *Int J Oncol*. 2017;50(2):365–372. doi:10.3892/ijo.2017.3834
108. Wang Q, Chen Y, Feng H, Zhang B, Wang H. Prognostic and predictive value of HURP in nonsmall cell lung cancer. *Oncol Rep*. 2018;39(4):1682–1692. doi:10.3892/or.2018.6280
109. Liu R, Guo CX, Zhou HH. Network-based approach to identify prognostic biomarkers for estrogen receptor-positive breast cancer treatment with tamoxifen. *Cancer Biol Ther*. 2015;16(2):317–324. doi:10.1080/15384047.2014.1002360
110. Fragoso MC, Almeida MQ, Mazzuco TL, et al. Combined expression of BUB1B, DLGAP5, and PINK1 as predictors of poor outcome in adrenocortical tumors: validation in a Brazilian cohort of adult and pediatric patients. *Eur J Endocrinol*. 2012;166(1):61–67. doi:10.1530/EJE-11-0806
111. Gomez CR, Kosari F, Munz JM, et al. Prognostic value of discs large homolog 7 transcript levels in prostate cancer. *PLoS One*. 2013;8(12):e82833. doi:10.1371/journal.pone.0082833
112. Kang MA, Kim JT, Kim JH, et al. Upregulation of the cycline kinase subunit CKS2 increases cell proliferation rate in gastric cancer. *J Cancer Res Clin Oncol*. 2009;135(6):761–769. doi:10.1007/s00432-008-0510-3
113. Tanaka F, Matsuzaki S, Mimori K, Kita Y, Inoue H, Mori M. Clinicopathological and biological significance of CDC28 protein kinase regulatory subunit 2 overexpression in human gastric cancer. *Int J Oncol*. 2011;39(2):361–372. doi:10.3892/ijo.2011.1056
114. Lan Y, Zhang Y, Wang J, Lin C, Ittmann MM, Wang F. Aberrant expression of Cks1 and Cks2 contributes to prostate tumorigenesis by promoting proliferation and inhibiting programmed cell death. *Int J Cancer*. 2008;123(3):543–551. doi:10.1002/ijc.23548
115. Shen DY, Zhan YH, Wang QM, Rui G, Zhang ZM. Oncogenic potential of cyclin kinase subunit-2 in cholangiocarcinoma. *Liver Int*. 2013;33(1):137–148. doi:10.1111/liv.12014
116. Wang JJ, Fang ZX, Ye HM, et al. Clinical significance of over-expressed cyclin-dependent kinase subunits 1 and 2 in esophageal carcinoma. *Dis Esophagus*. 2013;26(7):729–736.
117. Shen DY, Fang ZX, You P, et al. Clinical significance and expression of cyclin kinase subunits 1 and 2 in hepatocellular carcinoma. *Liver Int*. 2010;30(1):119–125. doi:10.1111/j.1478-3231.2009.02106.x
118. Kita Y, Nishizono Y, Okumura H, et al. Clinical and biological impact of cyclin-dependent kinase subunit 2 in esophageal squamous cell carcinoma. *Oncol Rep*. 2014;31(5):1986–1992. doi:10.3892/or.2014.3062
119. Yu MH, Luo Y, Qin SL, Wang ZS, Mu YF, Zhong M. Up-regulated CKS2 promotes tumor progression and predicts a poor prognosis in human colorectal cancer. *Am J Cancer Res*. 2015;5(9):2708–2718.